# Boron concentration profiling by high angle annular dark field-scanning transmission electron microscopy in homoepitaxial delta-doped diamond layers

Daniel Araújo, Maria de La Paz Alegre, José Carlos Pinero, Alexandre Fiori, Etienne Bustarret, François Jomard

# Boron concentration profiling by high angle annular dark field-scanning transmission electron microscopy in homoepitaxial $\delta$-doped diamond layers

D. Araújo,[1] M. P. Alegre,[1] J. C. Piñero,[1] A. Fiori,[2] E. Bustarret,[2] and F. Jomard[3]
[1]*Dpto Ciencia de los Materiales, Facultad de Ciencias, Universidad de Cádiz, 11510 Puerto Real (Cádiz), Spain*
[2]*Institut Néel, CNRS-Université Joseph Fourier, 25 av. des Martyrs, 38042 Grenoble, France*
[3]*Groupe d'Etude de la Matière Condensée (GEMaC), UMR 8635 du CNRS, UVSQ, 45 av. des Etats-Unis, 78035 Versailles Cedex, France*

(Received 14 June 2013; accepted 4 July 2013; published online 23 July 2013)

To develop further diamond related devices, the concentration and spatial location of dopants should be controlled down to the nanometer scale. Scanning transmission electron microscopy using the high angle annular dark field mode is shown to be sensitive to boron doping in diamond epilayers. An analytical procedure is described, whereby local boron concentrations above $10^{20}\,cm^{-3}$ were quantitatively derived down to nanometer resolution from the signal dependence on thickness and boron content. Experimental boron local doping profiles measured on diamond $p^-/p^{++}/p^-$ multilayers are compared to macroscopic profiles obtained by secondary ion mass spectrometry, avoiding reported artefacts. © *2013 AIP Publishing LLC*. [http://dx.doi.org/10.1063/1.4816418]

Intrinsically, diamond is one of the most promising materials for electronic devices. Its very high carrier mobility,[1,2] breakdown field,[3] saturation velocity, or thermal conductivity suit particularly well the requirements of high power and high velocity devices. However, other properties limit drastically the advent of this wide bandgap semiconductor in this technological field, such as mechanical properties (hardness and so on) or the difficulty in doping. In addition, the microstructural or chemical characterization of diamond is not straightforward.

Among the different approaches to diamond-based power devices, delta-doped structures were proposed for the fabrication[4,5] of MESFET. The idea was to reach high mobilities using carrier wave function delocalization away from the highly doped layer. In the case of diamond, a thickness below 5 nm would be required with very high doping levels ($p^{++}$ type, i.e., $>0.3$ at. % or $5\times10^{20}\,cm^{-3}$),[6] which are necessary to reach the insulator-to-metal transition.[7] For such applications, an accurate doping process and specific characterization methods should be developed, both in terms of doping level and localisation of boron acceptors.

Although early secondary ion mass spectroscopy (SIMS) profiles did not meet such requirements,[4] more recent Elastic Recoil Detection profiles have shown that the values mentioned above could be measured over a wide area.[8] The large dynamical doping range is a key advantage of SIMS to characterize such $\delta$-doped layers; in turn, it presents two important limitations:[9] (i) To avoid ion mixing inside the diamond crystal during SIMS operation, a non-trivial DRF (depth resolution function) deconvolution analysis is required, which strongly depends on the species at stake. (ii) The probed region extension averaged the deduced boron related profile. Doping level evaluation over micrometer-scale areas in diamond material can also be carried out by optical methods such as Raman[10] and FTIR.[11] Among these techniques, cathodoluminescence (CL)[12,13] is clearly the most sensitive[14] while ensuring a high spatial resolution since cross sectional analysis can be also carried out on FIB preparations.[15,16] However, the signal is too weak in heavily doped diamond to image the spatial distribution of dopants. The need of an imaging method able to quantify boron content and layer thickness becomes obvious when $\delta$-doped devices are being developed. For this reason, high angle annular dark field (HAADF[17] or Z-contrast mode) using a STEM (scanning transmission electron microscope) to thin homoepitaxial multilayers in order to determine the thickness, interface sharpness, and boron content of these doped structures is here applied. Recently, boron doping was also observed using this technique on nanocrystalline diamond.[18] Here, a modified method is applied to the case of boron $\delta$-doped layers in order to avoid FIB-lamella thickness effects. Comparison to SIMS experimental profile demonstrated the power of the method and showed that such layers are now close to reach the requirements for carrier delocalization.[6]

Two samples were studied: one multilayer stack including four thin (nominally 20–60 nm thick) and highly boron-doped homoepitaxial diamond layers (labelled sample A) to first show the method, and the other including only one boron $\delta$-doped layer (labelled sample B) to evidence the ultimate doping level and thickness that can be reached. The samples have been grown by MPCVD (Microwave Plasma Chemical Vapor Deposition) in a vertical silica tube reactor as described elsewhere[19] on a (100)-oriented HPHT (high pressure high temperature) type Ib diamond substrate. After a 2 h cleaning with pure hydrogen plasma at 880 °C, undoped ($p^-$) and heavily boron-doped ($p^{++}$) epilayers have been grown alternatively from respectively $H_2/He/CH_4/O_2$ and $H_2/He/CH_4/B_2H_6$ gas mixtures without turning off the plasma. For the purpose of this study, the $p^{++}$ epilayers of sample A have been labelled from #1 to #4 according to the growth sequence. As described in a previous work,[18] after the growth of each heavily $p^{++}$ layer, a specific etch-back procedure was performed during 3 min (#2), 6 min (#3), and 10 min (#4) using a mixture of hydrogen and oxygen in the plasma. The HAADF-STEM experiment was carried out in a Jeol 2010F microscope equipped with an annular dark field

 

(ADF) detector. To ensure high angle detection (HAADF), the camera length was fixed at 8 cm leading to minimum and maximum detector collection angles of 38.5 mrad and 99.8 mrad, corresponding to spatial frequencies $s$ around 4 and 1.5 $Å^{-1}$, respectively. The detector should be sensitive only above a $s_{min} = 1.5\ Å^{-1}$ threshold to avoid Bragg scattering effects. Because diamond is the hardest known material, specimen preparation for cross-section TEM observation was undertaken using a Focused Ion Beam in a Dual Beam Scanning electron microscope (FIB-Dual Beam, lift-off method).[20]

The use of the Z-contrast or HAADF-STEM mode is well known to allow atomic resolution.[21] For example, individual atoms at interfaces as isolated boron atoms in carbon nanostructures[22] or concentration profiles in nanostructures have been demonstrated. So far, the method has yielded either concentrations in the alloying range or individual atoms identification at atomic resolution, but seemed insufficiently sensitive for doping level determination in Si or III-V compounds. The low Z-number of carbon and the difference between the scattering cross sections of C and B at higher angles (about 30% at 100 mrad in our setup) made it possible to detect and image boron in the heavy doping range as shown in the following. Moreover such layers are visible by diffraction contrast or even in bright field condition with some slight defocus, but boron quantification is then very difficult.

Fig. 1(a) shows a HAADF-STEM micrograph with the four thin heavily boron doped $p^{++}$ layers embedded in an undoped ($p^{-}$) diamond layer. The darker tone at the right hand of the micrograph is due to a gradual reduction in thickness of the FIB lamella preparation, which is more marked close to the right-hand side. The convolution of thickness and chemical effects is well revealed in the intensity profile of Fig. 1(b), recorded along the 10 nm-wide line indicated on the micrograph. To separate both effects and analyse only the chemical concentration-related variation of the HAADF-STEM current intensity $I^{HAADF}$, an interpolation was performed using the data obtained only on the undoped region (in bold, i.e., taking off data of the heavily doped layers), and thus the ratio of the $I^{HAADF}(x)$ and $I^{HAADF}(0)$ where x is the boron content (i.e., current measured on the doped region and the corresponding current obtained by interpolation at the same position respectively) could be calculated at each position along the experimental profile. Then, at one specified position, the intensity difference between the doped (experimental value: $I^{HAADF}(x)$) and undoped (interpolated value: $I^{HAADF}(0)$) material was deduced independent of the sample preparation thickness, allowing determine the boron doping, thanks to the following simple modelization of $I^{HAADF}$.

According to the wave behavior of KeV electrons across a thin solid lamella, the ratio of scattered electrons depends on the square of the atomic scattering factor. In addition, interaction with phonons reduces the coherent intensity, and incoherent electrons are diffracted at high angles. Low angle scattering is dominated by elastic scattering as it results from Bragg reflections in the crystal, "Bragg scattering (BS)," while high angle scattering is dominated by inelastic scattering, i.e., incoherent scattering, which gives diffuse intensity

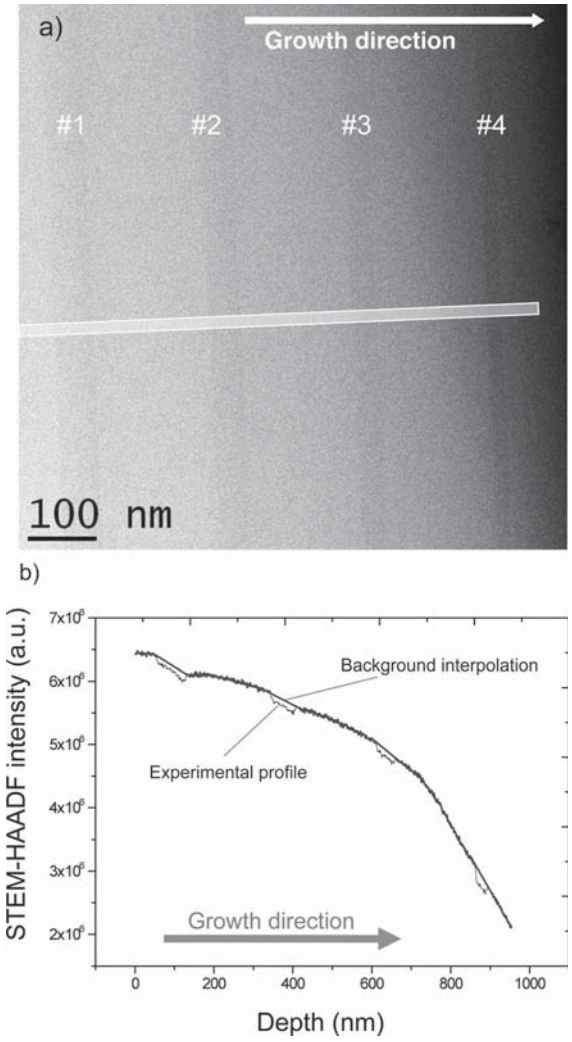


FIG. 1. (a) HAADF-STEM micrograph recorded on four "$\delta$-doped" layers. (b) Intensity profile recorded along the line indicated in the micrograph (black line) and the interpolation without taking into account the $\delta$-doped layers (bold curve). Difference between experimental values and interpolated ones allow to avoid the lamella TEM preparation thickness effects. To reduce signal-noise, an average of 100 profiles was carried out over the width of the line.

distribution, "thermal diffuse scattering (TDS)." Thus at sufficiently high angles there are no diffraction effects, and the scattered intensity depends directly on the square of the atomic scattering factor, $f(\theta)$, which gives the amplitude of the electron wave after scattering on one isolated atom. Then, the angular dependence of the electron emission writes

$$I^{HAADF}(s) = I_o\left[\sum_i |f_i(s)|^2\right] = I_o\left[\sum_{carbon} |f_{carbon}(s)|^2 + \sum_{boron} |f_{boron}(s)|^2\right], \quad (1)$$

where $I_o$ is the incident electron beam intensity, $f_i(s)$ is the atomic scattering factor for the atom i that depends on the scattering angle $\theta$ (=s/2) and have units of Å. For one species (i.e., i-subindex is either carbon or boron in Eq. (2)), using the atomic scattering factor values published by Kirkland[23] and integrating over the detector area in the reciprocal space (spatial frequencies $s$, *units of* $Å^{-1}$)

$$I_i^{HADDF} = \int_{s_{min,detector}}^{s_{max,detector}} [I_i^{HAADF}(s)]ds = I_0 N \times \sum_{s_{min,detector}}^{s_{max,detector}} f_{i,Kirkland}(s)^2 2\pi s\Delta s = I_0 N S_i, \quad (2)$$

where N is the number of atoms irradiated by the incident electron beam. The dependence of $f_{i,Kirkland}(s)$ over the range of the detector angle detection can be directly deduced from the values published by Kirkland[22] for either boron or carbon. In the case of the present experimental collection geometry, the calculation of sums labelled $S_i$ in Eq. (2) yielded for diamond and boron values of 0.0214 ($=S_{carbon}$) and 0.0153 ($=S_{boron}$). This corresponds to the probability for one incident electron to be scattered in the direction of the annular detector when scattering occurs either by a carbon or boron atom respectively. Considering that here a boron doped layer is observed, the electronic current scattered in the direction the annular detector by a doped layer is

$$I_x^{HAADF} = I_o N[(1-x)S_{carbon} + xS_{boron}], \quad (3)$$

x being the atomic proportion of boron in the diamond crystal. As the e-beam spot has a Gaussian shape in addition to have a not easily measurable current, it is difficult to determine precisely $I_0N$ (tentatively a value around $10^4$ nA was estimated). To deduce x, the ratio, R, between the current in the doped and undoped regions is evaluated

$$R = \frac{I^{HAADF}(x)}{I^{HAADF}(0)} = (1-x) + \frac{S_{boron}}{S_{carbon}}x. \quad (4)$$

Then the relative boron content writes as

$$x = \frac{1-R}{1-\frac{S_{boron}}{S_{carbon}}} = \frac{1-R_{measured}}{1-\frac{S_{boron}}{S_{carbon}}}C. \quad (5)$$

Therefore, the boron content can be determined by the ratio of electrons collected by the detector coming from doped and undoped regions. However, the factor R corresponds to the ratio of the electron currents scattered onto the detector and not on the current delivered by the detector ($R_{measured}$). In order to take into account this response, an experimental calibration of the used equipment has been carried out using a thick (4 $\mu$m) diamond homoepitaxial single layer, with a well-known doping level (obtained from a previous calibrated SIMS measurement[17]) at different thicknesses (controlled by the FIB related sample preparation) and different condenser apertures to vary the electron beam current. Brightness and contrast controls were kept at a fixed value (0 and 9, respectively) so that the correction factor C could be estimated for these experimental conditions.

Fig. 2 shows the result of applying Eq. (5) with this correction factor at each point of the profile shown in Fig. 1(b). The resulting doping profile indicates that boron is incorporated more easily close to undoped interfaces (see arrows). Since no extended defects could be detected by TEM on this preparation, this feature is tentatively attributed to the lattice strain gradient induced by the incorporation of boron. Indeed, a lattice expansion around 0.1% has been measured for a boron doping level of $10^{21}$ cm$^{-3}$.[24] As the observed noise was in the range of $10^{20}$ cm$^{-3}$, the dynamical range was limited to about one order of magnitude, so that the trend to obtain sharper interfaces upon longer etch-back steps,[19] although qualitatively confirmed, could not be inferred quantitatively from the data shown in Fig. 2.

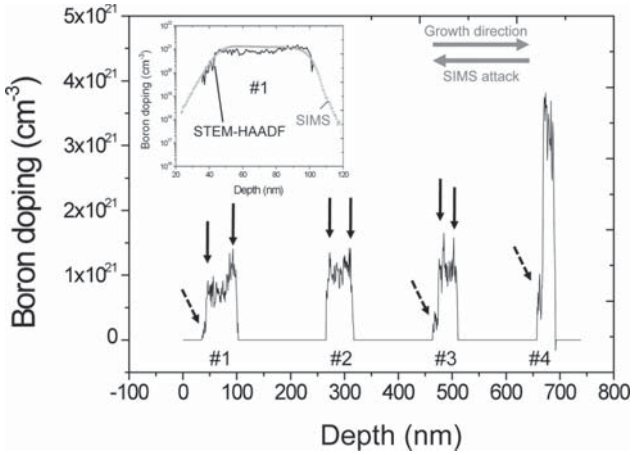


FIG. 2. Doping profile derived from Eq. (5) using the ratio between the measured and interpolated HAADF-STEM intensity along the experimental profile of Fig. 1(b). In the inset, comparison between the SIMS and HAADF-STEM profiles on layer #1 is represented. Note that the boron-scale is logarithmic to show the sensitivity of SIMS.

A more detailed comparison of the HAADF boron concentration profile of layers to SIMS profiles of the same sample confirmed the relevance of this (independent) calibration procedure for absolute concentrations, the agreement between SIMS and HAADF values being rather striking as shown in the inset for layer #1. Some local variations are revealed by the HAADF-STEM while SIMS averages the profile.

Another result was that the typical exponential profiles observed by SIMS over various orders of magnitude at the interfaces of the multilayer under study were probably an artefact, resulting from the ion-mixing generally involved

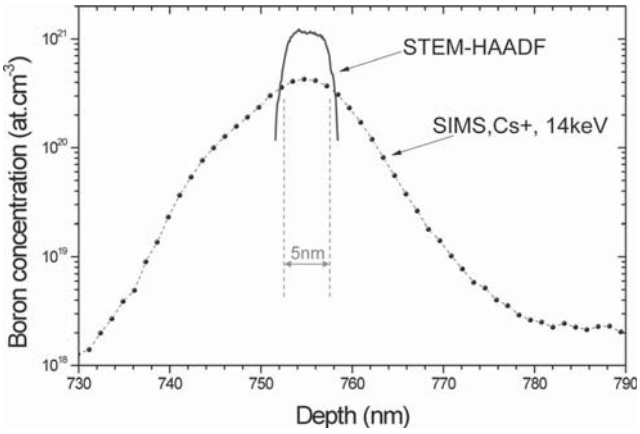


FIG. 3. Boron profiles in logarithmic scale obtained from SIMS and HAADF-STEM techniques on sample B. Ion-mixing is shown to broaden the SIMS profile. A 5 nm thick $\delta$-doped layer is demonstrated by the HAADF-STEM profile.

in SIMS measurements,[9–25] leading to systematic overestimates of the real width, similar to the case of silicon.[26] If this is the case, it is legitimate to ask how the layer thickness should be estimated from broadened SIMS profiles. Based on the comparison between the SIMS and HAADF-STEM profiles of several epilayers within various samples, the use of the extrema of the first derivative of the SIMS profile with respect to depth has been applied: the distance between these two extrema is usually within a few % of the thickness of the heavily doped epilayer as determined by HAADF-STEM. The fact that the latter profiles do not show any systematic broadening on one of the sides of the doped epilayers pointed to another probable consequence of ion-mixing: the ubiquitous enhancement of the width of the interface analysed after sputtering the $p^{++}$ region, which is apparent in most of the published SIMS profiles, is independent of how the samples were grown or whether the plasma was interrupted or not.

To illustrate the difference between both techniques on a very thin doped layer, HAADF-STEM and SIMS profiles are compared in Fig. 3 on a $\delta$-doped layer (sample B). Integration over a wider line allowed to reduce the HAADF-STEM noise with respect to that in Fig. 2. A logarithmic scale is used to show the high sensitivity of the SIMS, but, in contrast, ion-mixing is shown to broaden the recorded boron-profile. Note that for thicker layers (sample A) the difference is not so critical in contrast to thinner layers (#4 sample A and sample B). Such behavior motivated other authors to use complementary techniques to improve the SIMS profile; Chicot *et al.*[27] calculate this broadening to correct the experimental data while Balmer *et al.*[28] complete the SIMS data with elastic recoil detection analysis (ERDA) to estimate boron-doping thickness. Here, as a first result, a 5 nm-thick layer is demonstrated directly by the HAADF-STEM profile, showing that the growth technology is now close to reach quantum confinement enhancement of mobility.

In conclusion, boron content in-depth profiles of homoepitaxially grown heavily doped diamond epilayers were measured quantitatively by HAADF-STEM down to $10^{20}$ B/cm$^3$ at nanometric resolution. Boron was shown to locate preferentially at undoped/doped interface, and the broader SIMS profile of the deeper interface of $p^{++}$ layers is shown to be an artefact related to ion mixing processes. The experiments highlighted the potential of HAADF-STEM for characterizing, with a nanometric resolution, the boron content of diamond based delta-doped layers. Extremely thin $\delta$-doped layers down to 5 nm thick are demonstrated with in boron concentration edges steep enough to expect that even slightly thinner epilayers would induce some carrier delocalisation.

We would like to thank the Central Electron Microscopy Facilities of the University of Cádiz for technical support, the Ministerio de Ciencia e Innovación (MICINN) of the Spanish Government for funding under Grant No. TEC2009-11399, the Agence Nationale de la Recherche (France) for funding under Contract No. ANR08-BLAN-0195.

[1]J. Pernot, P. N. Volpe, F. Omnès, P. Muret, V. Mortet, K. Haenen, and T. Teraji, Phys. Rev. B **81**, 205203 (2010).
[2]P.-N. Volpe, J. Pernot, P. Muret, and F. Omnès, Appl. Phys. Lett. **94**, 092102 (2009).
[3]P.-N. Volpe, P. Muret, J. Pernot, F. Omnès, T. Teraji, Y. Koide, F. Jomard, D. Planson, P. Brosselard, N. Dheilly, B. Vergne, and S. Scharnholz, Appl. Phys. Lett. **97**, 223501 (2010).
[4]R. S. Balmer, I. Friel, S. M. Woollard, C. J. H. Wort, G. A. Scarsbrook, S. E. Coe, H. El-Hajj, A. Kaiser, A. Denisenko, E. Kohn, and J. Isberg, Philos. Trans. R. Soc. London, Ser. A **366**, 251 (2008).
[5]A. Denisenko and E. Kohn, Diamond Relat. Mater. **14**, 491 (2005).
[6]A. Fiori, J. Pernot, E. Gheeraert, and E. Bustarret, Phys. Status Solidi A **207**, 2084 (2010).
[7]T. Klein, P. Achatz, J. Kačmarčik, C. Marcenat, F. Gustafsson, J. Marcus, E. Bustarret, J. Pernot, F. Omnès, B. E. Sernelius, C. Persson, A. Ferreira da Silva, and C. Cytermann, Phys. Rev. B **75**, 165313 (2007).
[8]H. El Hajj, A. Denisenko, A. Bergmaier, G. Dollinger, M. Kubovic, and E. Kohn, Diamond Relat. Mater. **17**, 409 (2008).
[9]A. Fiori, F. Jomard, T. Teraji, S. Koisumi, J. Isoya, E. Gheeraert, and E. Bustarret, Appl. Phys. Express **6**, 45801 (2013).
[10]M. Bernard, A. Deneuville, and P. Muret, Diamond Relat. Mater. **13**, 282–286 (2004).
[11]C. Fernandez-Lorenzo, D. Araujo, J. Martin, R. Alcantara, J. Navas, M. P. Villar, M. P. Alegre, P. N. Volpe, F. Omnès, and E. Bustarret, Diamond Relat. Mater. **19**, 904 (2010).
[12]A. Deneuville, C. Baron, S. Ghodbane, and C. Agnès, Diamond Relat. Mater. **16**, 915 (2007).
[13]J. Barjon, P. Desfonds, M.-A. Pinault, T. Kociniewski, F. Jomard, and J. Chevallier, J. Appl. Phys. **101**, 113701 (2007).
[14]F. Omnès, P. Muret, P.-N. Volpe, M. Wade, J. Pernot, and F. Jomard, Diamond Relat. Mater. **20**, 912 (2011).
[15]D. Araújo, M. P. Alegre, A. J. García, P. Villar, E. Bustarret, P. Achatz, P. N. Volpe, and F. Omnès, Phys. Status Solidi C **8**, 1366 (2011).
[16]D. Araújo, M. P. Alegre, A. J. García, J. Navas, M. P. Villar, E. Bustarret, P. N. Volpe, and F. Omnès, Diamond Relat. Mater. **20**, 428 (2011).
[17]D. Araújo, P. Achatz, R. El Bouayadi, A. J. Garcia, M. P. Alegre, M. P. Villar, F. Jomard, and E. Bustarret, Diamond Relat. Mater. **19**, 972 (2010).
[18]Y.-G. Lu, S. Turner, J. Verbeeck, S. D. Janssens, P. Wagner, K. Haenen, and G. V. Tendeloo, Appl. Phys. Lett. **101**, 41907 (2012).
[19]A. Fiori, T. N. T. Thi, G. Chicot, F. Jomard, F. Omnès, E. Gheeraert, and E. Bustarret, Diamond Relat. Mater. **24**, 175 (2012).
[20]J. S. Park, R. Sinclair, D. Rowcliffe, M. Stern, and H. Davidson, J. Mater. Sci. **41**, 4611 (2006).
[21]J. Pizarro, P. L. Galindo, E. Guerrero, A. Yáñez, M. P. Guerrero, A. Rosenauer, D. L. Sales, and S. I. Molina, Appl. Phys. Lett. **93**, 153107 (2008).
[22]U. Bangert, M. H. Gass, A. L. Beloch, R. R. Nair, and J. Eccles, in SBDD XIV Diamond Workshop, March 2009, Hasselt, Belgium.
[23]E. J. Kirkland, R. F. Loane, and J. Silcox, Ultramicroscopy **23**, 77 (1987).
[24]T. Wojewoda, P. Achatz, L. Ortéga, F. Omnès, C. Marcenat, E. Bourgeois, X. Blase, F. Jomard, and E. Bustarret, Diamond Relat. Mater. **17**, 1302 (2008).
[25]S. Hoffmann, Appl. Phys. **13**, 205 (1977).
[26]A. Takano, Y. Homma, Y. Higashi, H. Takenaka, S. Hayashi, K. Goto, M. Inoue, and R. Shimizu, Appl. Surf. Sci. **203–204**, 294 (2003).
[27]G. Chicot, T. N. T. Thi, A. Fiori, F. Jomard, E. Gheeraert, E. Bustarret, and J. Pernot, Appl. Phys. Lett. **101**, 162101 (2012).
[28]R. S. Balmer, I. Friel, S. Hepplestone, J. Isberg, M. J. Uren, M. L. Markham, N. L. Palmer, J. Pilkington, S. Majdi, and R. Lang, J. Appl. Phys. **113**, 33702 (2013).